First posted online on 18 March 2020 as 10.1242/dmm.043513
Access the most recent version at http://dmm.biologists.org/lookup/doi/10.1242/dmm.043513

The transcription factor Nurr1 is up-regulated in Amyotrophic Lateral Sclerosis patients and SOD1-G93A mice

Summary statement: The transcription factor Nurr1 in ALS pathology

Valeria Valsecchi[a,b,c*], Marina Boido[a,b*], Francesca Montarolo[b,d], Michela Guglielmotto[a,b], Simona Perga[a,b,d], Serena Martire[b,d], Santina Cutrupi[e], Andrea Iannello[e], Nadia Gionchiglia[b], Elena Signorino[b], Andrea Calvo[f,g], Giuseppe Fuda[f,g], Adriano Chiò[f,g], Antonio Bertolotto[b,d] and Alessandro Vercelli[a,b]

[a]Department of Neuroscience Rita Levi Montalcini, University of Turin, via Cherasco 15, 10126, Turin, Italy.
[b] Neuroscience Institute Cavalieri Ottolenghi (NICO), University of Turin, Regione Gonzole 10, 10043, Orbassano, Turin, Italy.
[c]Department of Neuroscience, Reproductive and Dentistry Sciences, University of Naples "Federico II", via S.Pansini 5, 80131, Naples, Italy.
[d] Neurobiology Unit, Neurology - CReSM (Regional Referring Center of Multiple Sclerosis), AOU San Luigi Gonzaga, Regione Gonzole 10, 10043, Orbassano, Turin, Italy.
[e]Department of Clinical and Biological Sciences, University of Turin, Regione Gonzole 10, 10043, Orbassano (TO), Italy
[f]Department of Neuroscience Rita Levi Montalcini, Amyotrophic Lateral Sclerosis Expert Center (CRESLA), University of Turin, via Cherasco 15, 10126, Turin, Italy.
[g]University Hospital Città della Scienza e della Salute, corso Bramante 88, 10126, Turin, Italy

*These two authors equally contributed

Correspondence should be addressed to:

Valeria Valsecchi, PhD

Department of Neuroscience Rita Levi Montalcini, University of Turin, via Cherasco 15, 10126, Turin, Italy and Neuroscience Institute Cavalieri Ottolenghi (NICO), University of Turin, Regione Gonzole 10, 10043, Orbassano, Italy.

Current address:

Department of Neuroscience, Reproductive and Dentistry Sciences, University of Naples "Federico II", Via S.Pansini 5, 80131, Naples, Italy.

e-mail: valsecchiv@yahoo.com

Email addresses: marina.boido@unito.it; francesca.montarolo@unito.it; michela.guglielmotto@unito.it; simona.perga77@gmail.com; serena.martire@gmail.com; santina.cutrupi@unito.it; iannellochoc@gmail.com; nadia.gionchiglia@gmail.com; elena.signorino@gmail.com; andrea.calvo@unito.it; gio.fuda@gmail.com; adriano.chio@unito.it; antonio.bertolotto@gmail.com; alessandro.vercelli@unito.it

Keywords

ALS, SOD1-G93A mice, motor neuron disease, neuroinflammation, Nurr1

ABSTRACT

Amyotrophic lateral sclerosis (ALS) is a neurodegenerative disease that affects both lower and upper motor neurons (MNs) in the central nervous system (CNS). ALS etiology is highly multifactorial and multifarious, and an effective treatment is still lacking. Neuroinflammation is a hallmark of ALS and could be targeted to develop new therapeutic approaches. Interestingly, the transcription factor Nurr1 has been demonstrated to play an important role in inflammatory process in several neurological disorders, such as Parkinson's disease (PD) and Multiple Sclerosis (MS).

In the present paper, we demonstrated for the first time that Nurr1 expression levels were up-regulated in the peripheral blood of ALS patients. Moreover, we investigated Nurr1 function in the SOD1-G93A mouse model of ALS. Interestingly, Nurr1 was strongly up-regulated in the spinal cord during the asymptomatic and early symptomatic phases of the disease, where it promoted the up-regulation of the BDNF mRNA and the repression of NF-kB pro-inflammatory targets, such as iNOS. Therefore, we hypothesize that Nurr1 is activated in an early phase of the disease as survival endogenous anti-inflammatory mechanism, although not sufficient to revert disease progression.

Based on these observations, Nurr1 could represent a potential biomarker for ALS and a promising target for future therapies for ASL.

INTRODUCTION

Amyotrophic lateral sclerosis (ALS) is a neurodegenerative disease that affects both lower motor neurons (MNs) in brainstem and spinal cord, and upper MNs in the cerebral cortex (Pasinelli and Brown, 2006). Loss of these neurons leads to muscle weakness and paralysis and ultimately to death due to respiratory failure 2-5 years after diagnosis (Worms et al., 2001). The incidence is about one-to-two individuals per 100,000 per year, with males being affected more frequently than females (Robberecht and Philips, 2013). The 90% of cases are classified as sporadic (sALS) and the remaining 10% as familial (fALS) with a Mendelian pattern of inheritance. Gene mutations in fALS are in several genes: the copper/zinc superoxide dismutase 1 (SOD1), the trans active response DNA binding protein (TARDBP), the fused in sarcoma/translocated in liposarcoma (FUS/TLS) and the chromosome 9 open reading frame 72 (C9orf72), that contribute for the two-third of fALS and approximately for the 10% of sALS, whereas for the others the etiology is unknown (Renton et al, 2014; Chia et al., 2018). The clinical phenotype of fALS is usually indistinguishable from sALS and an effective therapy is still elusive.

ALS etiology is multifarious and has been associated to mitochondrial dysfunction and oxidative stress, excitotoxicity, deficits in axonal architecture/function and protein quality control, protein misfolding and aggregation, loss of neurotrophic factors, dysregulation of RNA metabolism and inflammation (Ferraiuolo et al, 2011; Cozzolino et al., 2012). In particular, neuroinflammation is a common hallmark of neurodegenerative diseases, such as ALS but also Parkinson's disease (PD). Indeed, in ALS, a dramatic activation of microglia, astrocytes and complement system is reported, contributing to neurodegeneration partly due to up-regulation of inflammatory genes (Haidet-Phillips et al, 2011). In addition, the role of adaptive immune system modulates the balance between neuroprotection and neurotoxicity (Thonhoff et al., 2018). The effects on CNS and peripheral blood changes at several phases of disease and regulatory T cells dysregulation act on disease outcome (Henkel et al., 2013). Thus, seen the central contribution of neuroinflammation to ALS pathogenesis, nowadays the identification of novel therapeutic targets acting on inflammation is mandatory (Troost et al, 1990; Zhao et al, 2013).

In this scenario, an interesting role is played by the Nuclear receptor related-1 protein Nurr1, also called NR4A2. Nurr1 is an orphan receptor belonging to the Nuclear receptor subfamily 4 group A (NR4A) family, including the Nerve growth factor IB (NGFIB, Nur77, NR4A1) and the Neuron derived orphan receptor 1 (NOR-1, NR4A3). In CNS, Nurr1 has a well-established role in the development and the maintenance of midbrain dopaminergic (mDA)

neurons (Zetterstrom et al.,1997; Saucedo-Cardenas et al., 1998). Given its crucial functions, altered Nurr1 expression is implicated in dopamine-associated brain disorders, including PD. Notably, Nurr1 expression level in mDA neurons decreases in PD patients (Hering et al, 2004) and single nucleotide polymorphisms (SNPs) and mutations resulting in reduced expression of Nurr1 are associated with familial and sporadic forms of PD.

Interestingly, Nurr1 is a constitutively active transcription factor binding its target genes as a monomer, homodimer or heterodimer in association with retinoid X receptors (RXRs) (Aarnisalo et al., 2002; Maira et al., 1999; Wang et al., 2003). In murine models of PD the role of Nurr1 emerged both in neuro-protection and immunomodulation. Indeed, Nurr1 plays an anti-inflammatory role inhibiting the expression of the pro-inflammatory genes of the NF-kB pathway in microglia and astrocytes (Saijo et al., 2009). Specifically, knocking-down Nurr1 in mice leads to an increased activation of glial cells exposed to lipopolysaccharide (LPS), with subsequent production of higher levels of inflammatory cytokine-encoding mRNAs and neurotoxic effector proteins such as Tumor necrosis factor-α (TNF-α), inducible nitric oxide synthase (iNOS) and interleukin 1β (IL-1β), responsible for inflammation-induced neuronal death (Saijo et al., 2009, McMorrow and Murphy, 2011). In addition, Nurr1 induces the expression of neurotrophic factors such as brain-derived neurotrophic factor (BDNF) (Barneda-Zahonero et al., 2012).

Besides its role in CNS, Nurr1 is an active player of PD, since down-regulated gene expression levels were also found in peripheral blood obtained from PD patients with progressive loss of mDA neurons (Le et al, 2008; Liu et al, 2012; Montarolo et al., 2016).

Recently, it has been demonstrated that Nurr1 also controls the expression of several nuclear-encoded mitochondrial genes involved in oxidative respiration such as SOD1, Ts translation elongation factor (TSFM) and cytochrome C oxidase subunit 5β (COX5β), exerting an important role to sustain the respiratory function (Kadkhodaei et al., 2013). Therefore, we first analyzed the Nurr1 gene expression level in blood obtained from ALS patients in comparison to healthy controls (HC). Then, to better understand its role in ALS, we investigated its expression and function in a murine model of ALS, the SOD1-G93A mouse.

RESULTS

Nurr1 mRNA is up-regulated in the peripheral blood of ALS patients

Gene expression analysis of Nurr1 was performed on whole peripheral blood obtained from 43 ALS patients and 41 HC subjects, whose demographic and clinical characteristics are summarized in Table 1. In particular, ALS group, composed by 7 fALS and 36 sALS patients, showed higher Nurr1 mRNA levels compared to HC (Fig.1A). Furthermore, there was a significant difference in age (t-test, p=0.002, Table 1) but not in gender between ALS patients and HC (Fisher exact test, p=0.38). In order to assess potential bias related to age, the correlation between age and gene expression levels of Nurr1 was evaluated in HC subjects and no significant results were highlighted, as previously reported by Montarolo and colleagues (Montarolo et al., 2016) (Pearson correlation coefficient r=0.13, p=0.41). Also correlation analyses between Nurr1 gene expression of ALS patients and age at the time of sampling (Pearson correlation coefficient r=-0.09, p=0.55) (Fig.S1A) and age at disease onset (Pearson correlation coefficient r=-0.16, p=0.31) did not highlight significant results. Similarly, there are no significant differences in Nurr1 expression between genders in both HC (t-test, p=0.53) and ALS patients (Mann-Whitney U test, p=0.32) (Fig.S1B). The influence on Nurr1 expression level of the pharmacological treatment indicated in Table 1, was not assessed due to the small sample size of each group. Interestingly, among fALS patients, 4 carried mutations in C9Orf72, 2 in SOD1 gene and 1 in TARDBP gene, whereas 3 sALS patients carried mutations in C9Orf72, SOD1 and in OPTN genes. We also reported Nurr1 expression levels for the different groups (Fig.S1C).

Nurr1 mRNA and protein are up-regulated in the spinal cord of SOD1-G93A mice in the asymptomatic and early symptomatic phases of the disease

The high levels of Nurr1 expression in samples of peripheral blood in ALS patients suggested a potential role in ALS pathogenesis. In order to investigate the role of Nurr1 in ALS outcome, we used a mouse model of ALS, the SOD1-G93A (TG). This model owns a high copy number of the transgene, and it is one of the most commonly used (Gurney et al., 1994). Male mice develop the first symptoms of the disease approximately at 3 months of age and die in about 4 weeks after disease onset. Behavioral tests such as Rotarod and Paw Grip Endurance (PaGE) were used to evaluate the appearance of the first motor deficits and to divide the animals in three experimental groups: i) asymptomatic mice; ii) early symptomatic mice; iii) late symptomatic mice (Boido et al., 2014). Age-matched wild type (WT) male mice were used as controls. Female animals were excluded from the study, due

to significant differences observed in female compared to male TG animals, probably for an estrogen neuroprotective effect (Vercelli et al., 2008).

First, we measured Nurr1 mRNA levels in the whole peripheral blood obtained from early and late symptomatic TG animals, considered as a single group. The analysis revealed no differences in Nurr1 expression level in TG compared to age-matched WT mice (Fig.1B). On the contrary, by evaluating Nurr1 expression levels in the spinal cord of TG mice (Fig2A-B), we observed that Nurr1 mRNA was significantly up-regulated, up to 2.2-fold, in the asymptomatic phase of the disease, compared to respective controls. In the early symptomatic phase of the disease, Nurr1 mRNA content was still higher than WT animals with a slightly lesser extent (1.8-fold), while in end stage mice Nurr1 mRNA levels were not different to age-matched WT ones (Fig.2A).

Nurr1 protein levels in nuclear extracts obtained from the spinal cord of TG mice confirmed the results obtained with mRNA. In particular, Nurr1 protein was strongly up-regulated of 3.6 and 2.6-fold in the nuclei of asymptomatic and early symptomatic TG mice, respectively, compared to WT controls (Fig.2B). On the contrary, WT animals presented comparable levels of Nurr1, both at mRNA and protein levels in all groups analyzed (Fig.2A-B).

Nurr1 is able to activate BDNF expression and to prevent NF-kB target gene activation in the asymptomatic phase of the disease of SOD1-G93A mice

Next, we investigated the possible role exerted by Nurr1, by comparing TG and WT spinal cord samples. Since it has been demonstrated that the transcription factor Nurr1 can directly activate its target genes, such as BDNF (Barneda-Zahonero et al., 2012), we performed a real time-PCR analysis for BDNF. Furthermore, Nurr1 can dock on p65, the NF-kB trans-activating subunit, blocking the activation of its pro-inflammatory genes, such as iNOS (Saijo et al., 2009; De Miranda et al., 2015). Therefore, in order to investigate whether Nurr1 was involved in NF-kB pathway, we measured iNOS mRNA and performed chromatin immunoprecipitation assay following q-PCR (ChIP-qPCR) on iNOS promoter using antibodies against Nurr1 or p65.

Our results showed a significant increase in BDNF mRNA levels in the asymptomatic phases of the disease (Fig.3A). In particular, a significant increase up to 1.8-fold was observed in asymptomatic TG animals compared to WT. In early symptomatic mice, BDNF levels were still higher than respective controls, but not significantly (1.5-fold). In a late phase of the disease, BDNF levels were comparable to respective WT controls.

On the other hand, we observed a down-regulation of iNOS mRNA in the asymptomatic phases of the disease up to 40%, compared to age matched WT animals, that was no longer

reported in early symptomatic mice. Furthermore, in a late phase of the disease iNOS mRNA was strongly up-regulated up to 4.3-fold in TG animals compared to respective controls (Fig.3B).

In order to assess whether iNOS modulation depended on a direct competition between Nurr1 and NF-kB binding on its promoter, we performed ChIP-qPCR assay (Fig.3C). In particular, in asymptomatic animals Nurr1 binding, expressed as TG to WT ratio, was 2.2-fold higher in TG compared to age-matched WT animals. Interestingly, at this age Nurr1 binding was 4.6-fold higher compared to p65 binding on iNOS promoter. Furthermore, during disease progression Nurr1 binding decreased, mirrored by a parallel increase of p65 binding. In particular, in late symptomatic TG animals p65 binding was 2.8-fold higher than WT, and TG/WT ratio of p65 binding was 2.6-fold higher compared to Nurr1 (Fig.3C). Finally, we performed ChIP-qPCR assay on iNOS promoter using antibody against tri-methylation at lysine 4 of histone H3 (H3K4me3) and tri-methylation at lysine 27 of histone H3 (H3K27me3), markers for active and repressive genes, respectively (Kim, et al., 2013). Interestingly, our results showed that H3K4me3 enrichment increased 4.2-fold compared to H3K27me3, suggesting that iNOS promoter is active in according with increased iNOS mRNA levels (Fig.3B).

Nurr1 protein is expressed in motor neurons and, to a less extent, in astrocytes of SOD1-G93A mice

In order to investigate in which CNS cell types Nurr1 was expressed, representative double immunofluorescence experiments were performed in spinal cord sections with antibodies against i) the neurofilament H (SMI-32), a specific marker for MNs, ii) the glial fibrillary acidic protein (GFAP), an intermediate filament protein expressed mainly by astrocytes in the CNS, and iii) CD68 protein, that is highly expressed by macrophages and activated microglia.

In particular, for the first time, we observed that Nurr1 is physiologically expressed in the cytoplasmic compartment of SMI32 positive cells of WT animals, indicating Nurr1 presence in MNs (Fig4.A, panels a''-a''' thin arrows). Interestingly, in asymptomatic and early symptomatic TG mice, Nurr1 expression was mainly evident in the nuclear compartment of MNs (Fig.4A, panels b''-b''', c''-c''' thick arrows), in agreement with its up-regulation in nuclear extract observed with WB analysis. By contrast, in late symptomatic TG animals, Nurr1 immunostaining was still present only in MN cytoplasm (Fig.4A, panels d''-d''' thin arrows).

Furthermore, since neuroinflammation is a characteristic hallmark of ALS (see Fig.S1 and S2, in agreement with Ilieva et al., 2009; Boido et al., 2014; Anzilotti et al., 2018) and, in addition, Nurr1 is reported to play an anti-inflammatory role in astrocytes and microglial cells

(Saijo et al, 2009), we investigated its expression respectively in GFAP- and CD68-positive cells.

Double immunofluorescence staining with GFAP and Nurr1 revealed that Nurr1 immunosignal was present in the nuclear compartment of rare astrocytes cells at early stages of the disease (Fig.5A, panels a''-a''', thick arrows), while it was absent in late symptomatic phase (Fig.5A, panels b''-b''').

On the other hand, double immunostaining with CD68 and Nurr1 did not highlight Nurr1 expression in CD68 positive cells (Fig.5B, panels c''-c''', d''-d''').

DISCUSSION

In the present paper, for the first time, we investigated the expression of the transcription factor Nurr1 in blood obtained from ALS patients and in blood/spinal cord of a murine model of ALS, the SOD1-G93A mouse.

As known, Nurr1 plays an important role in the maturation of mDA neurons (Kadkhodaei et al., 2009), linking its deficiency mainly to PD. In fact, several human mutations in the gene encoding for Nurr1 protein, the *NR4A2* gene, are associated with late-onset familial PD (Le et al., 2003), and the SNPsrs35479735 (insertion/deletion of a G) seems to be a significant risk factor for the development of PD (Liu et al., 2017; Ruiz-Sánchez et al., 2017). Furthermore, Nurr1 gene expression level is down-regulated in blood of PD patients with progressive loss of DA neurons (Le et al, 2008; Liu et al, 2012; Montarolo et al., 2016). Moreover, conditional ablation of Nurr1 in adult mature mDA neurons in mice shows down-regulation of several genes involved in oxidative respiration, and particularly of SOD1 (Kadkhodaei et al., 2013), a key enzyme in ALS disease (Renton et al., 2014; Chia et al., 2018) that prompted us to explore the functional role of Nurr1 in ALS pathology.

Notably, in the whole blood obtained from ALS patients we highlighted a significant increase in mRNA levels of Nurr1 compared to HC. Nurr1 has a central role in immune homeostasis, where is able to regulate induction, maintenance and suppressor functions of regulatory T cells (Tregs). In particular, it represses the aberrant Th1 induction through transcriptional activation of the master transcription factor of Treg cells, the forkhead transcription factor (*Foxp3*) and by inhibiting the cytokine interferon γ (IFNγ) and interleukin-17 (IL-17) production (Sekiya et al., 2011; 2013). Therefore, Nurr1 mRNA up-regulation in ALS blood patients suggested an important role of this transcription factor also in ALS, in which immune cells are able to exert either a detrimental or a protective action on MN survival (Chiu et al., 2008; Hooten et al., 2015). Indeed, convincing evidence report that ALS is a systemic

disorder characterized by peripheral immune alterations (McCauley and Baloh, 2019). Autopsy from ALS patients showed modifications in the frequency of circulating immune cell populations and in the cytokines expression (Zhang et al., 2005; McCombe and Henderson, 2011; Murdock et al., 2017). However, the peripheral mechanism that critically contributes to the ALS disease process and whether it represents a consequence or play a causative role is still unclear. Nurr1 up-regulation could be driven by a response to tissue damage in the brain, initially sensed by resident glia then amplified and propagated by the peripheral immune cells or by an intrinsically altered peripheral immune system in ALS patients. Indeed, Nurr1 expression has been reported in dendritic cell (Saini et al., 2016), T-cell (Sekiya et al., 2011; Won and Hwang, 2016) and in macrophages (Bonta et al., 2006).

In order to shed light on the role of Nurr1 in ALS pathology, we then investigated Nurr1 expression and its mechanism of action in the SOD1-G93A mouse, one of the most used ALS murine model. In particular, we assessed Nurr1 expression level in the blood of early and late symptomatic animals, considering them a unique group to better represent ALS patient sampling. However, Nurr1 expression in TG mice blood did not reveal a significant increase compared to age-matched WT animals, in contrast with the increase observed in ALS patients. This discrepancy is probably due to the small sample size and/or to the not parallel phases of disease between the human ALS and the murine model. Furthermore, our mouse model carried the mutation in the SOD1 gene that represents only the 7% of our ALS patient cohort.

On the contrary, in the spinal cord of TG mice our data revealed that Nurr1 was strongly up-regulated in the early phases of the disease in TG mice, where it i) translocated into the nuclei of MNs and (to a less extent) astrocytes, ii) induced neurotrophic factor BDNF expression, and iii) inhibited iNOS expression by docking to NF-kB on iNOS promoter. The above mentioned observations have been obtained by RT-PCR, WB, ChIP-qPCR assay, and immunofluorescence (IF) analysis. Concerning IF experiments, Nurr1 antibody is mostly used in immunocytochemistry (Zhou et al., 2010; Lee et al., 2012; Alvarez-Castelao et al., 2013), whereas, on tissue samples, it tends to give an undesired noisy background (Baron et al., 2012; Garcia-Perez et al., 2013), despite the antigen retrieval passage. However, we are quite confident about the labeling specificity, since its recalls the molecular trend observed with RT-PCR and WB assays.

Our results for the first time highlighted Nurr1 expression in spinal cord MNs. Indeed, Nurr1 was physiologically present in the cytoplasmic compartment of MNs from WT animal, suggesting a potential role of this transcription factor for the survival of cholinergic neurons, that are affected in this neurodegenerative disease. Notably, very early during disease

progression, in asymptomatic and early symptomatic phases, Nurr1 was up-regulated at transcriptional level as suggested by RT-PCR analysis. Following activation, Nurr1 was translocated to the nucleus as indicated by its increased levels in nuclear extract of TG mice, mainly in MNs and rarely in astrocytes as indicated by IF experiments. Within the nuclei of asymptomatic animals, Nurr1 was able to activate the BDNF, its target gene, and to repress the transcription of iNOS. Indeed, Nurr1 up-regulation in the asymptomatic phase of the disease was accompanied by an increase in BDNF mRNA and a reduction of iNOS mRNA, as demonstrated by RT-PCR assay. iNOS repression was likely due to a direct competition between Nurr1 and NF-kB on iNOS promoter as indicated by ChIP-qPCR assay, in agreement with the mechanism of action proposed by Sajio and coworkers for Parkinson's disease (Saijo et al., 2009). However, in the early symptomatic phase, even if Nurr1 levels were higher in the nuclear compartment of TG mice compared to age-matched WT, it was not able to activate BDNF or repress iNOS. Finally, in late symptomatic animals, when Nurr1 was no longer up-regulated at transcriptional levels and apparently absent from nuclear compartments, we observed a strong binding of NF-kB to iNOS promoter and an enrichment of H3K4me3, indicating active gene in according with increase of its mRNA levels.

Therefore, we hypothesized that Nurr1 is not directly involved in the development of ALS pathology, but may very likely act as an endogenous mean to delay the pathogenetic mechanisms. In particular, Nurr1 could be activated before symptoms onset, as endogenous neuroprotective mechanism in order to exert an anti-inflammatory role, although not sufficient to revert disease progression. Moreover, preventing the final downregulation of Nurr1 and exploiting its ability to activate BDNF and to repress iNOS in the late stages of disease could represent a useful therapeutic tool.

Interestingly, Nurr1 has recently emerged to play a key role in the mediation of the inflammatory responses in a cell type-specific manner in several diseases such as cancer, immune alterations, metabolic, cardiovascular, or neurological diseases (Rodríguez-Calvo et al., 2017; Safe et al., 2016). In particular, Saijo and coworkers demonstrated that Nurr1 exerts an important anti-inflammatory role following microglial activation induced by lipopolysaccharide (LPS) injection limiting the production of neurotoxic mediators by glial cells and protecting DA neurons from inflammation (Saijo et al., 2009). Furthermore, a neuroprotective effect of Nurr1 was also demonstrated in the Multiple Sclerosis (MS) murine model, represented by EAE (Experimental Autoimmune Encephalomyelitis). Indeed, it has been demonstrated that a preventive treatment with the Nurr1 activator isoxazolo-pyridinone 7e (IP7e) delays onset and reduces the incidence and the severity of EAE, reducing

inflammation in the spinal cord of treated mice probably through an NF-kB dependent mechanism (Montarolo et al., 2014).

Interestingly, Nurr1 is able to protect hippocampal neurons within the CA1 field following kainic acid insult in mice (Volakakis et al., 2010) and emerged also as mediator of CREB-dependent neuroprotection in mouse embryonic stem cell-derived neurons (Volakakis et al., 2010).

On the other hand, Nurr1, and more in general NR4A family members, are also described as pro-inflammatory factors with controversial results in several disease models (Rodriguez-Calvo et al., 2017).

Conclusions

Collectively, our results demonstrated for the first time that Nurr1 mRNA is up-regulated in blood samples of ALS patients, therefore, we speculate that it could be considered a biomarker candidate for ALS. However, further studies will be necessary to confirm this aspect and the specific role of Nurr1 in the peripheral immune system during disease progression.

In addition, we demonstrated in a mouse model of ALS that Nurr1 is activated in the early symptomatic phase of the disease, probably as a neuroprotective endogenous mechanism, in agreement with the current hypothesis supporting an initial activation of glial cells aimed to sustain MNs viability through neurotrophic factors (IGF-1), anti-inflammatory interleukins (IL-4, IL10), and cytokines secretion (Chiu et al., 2008; Henkel et al., 2009; Murdock et al., 2015; Hooten et al., 2015). Later on during disease progression, we observed the inactivation of Nurr1, that was no longer up-regulated at mRNA level, was absent from the nuclear compartment and was unable to dock NF-kB on iNOS promoter. Therefore, we speculate that Nurr1 might represent a promising target for ALS therapy, seen that neuroinflammation is a relatively unexplored field that can modify the course of ALS disease. Further studies augmenting the anti-inflammatory effect through Nurr1 activation could mitigate the toxic environment, modulate neuroinflammation, and foster MN repair process, giving a positive impact for ALS treatment.

MATERIALS AND METHODS

Enrolled subjects

Forty-three patients affected by ALS and forty-one healthy controls (HC) were enrolled in the current study. ALS patients were followed and clinically monitored by neurologist of the ALS Expert Center (CRESLA), 'Città della Scienza e della Salute', University Hospital, Turin. Most of the ALS patients received disease-specific drugs at the time of blood sampling, such as riluzole alone or combined with symptomatic therapies. HC recruited from volunteers, were asked to complete a health questionnaire to exclude any acute or chronic inflammatory and neurological disease. All the subjects enrolled in the study were from Caucasian origin. Demographic and clinical features of patients and HC are summarized in Table 1.

This study was approved by Piedmont and San Luigi University Hospital Ethical Committee (N°80/2011, May 25th, 2011) and was conducted in accordance with the ethical standards laid down in the 1964 Helsinki declaration and its later amendments. Written informed consent was obtained from all individual participants included in the study at the time of blood drawing.

Animal care and use

Experiments were performed on male transgenic mice B6SJL-TgN(SOD1G93A)1Gur over-expressing human SOD1, containing the Gly93 to Ala mutation (Jackson Laboratory, stock number 002726); these mice have high transgene copy number, as reported in the datasheet. The colony was derived by breeding male transgenic (TG) mice to naive (B6xSJL/J)F1 females (WT) (Janvier SAS). Overall, 35 WT and 35 TG mice, housed under diurnal lighting conditions (12 h darkness/light) were used. All experimental procedures on live animals were carried out in strict accordance to the European Communities Council Directive 86/609/EEC (November 24, 1986) Italian Ministry of Health and University of Turin institutional guidelines on animal welfare [law 116/92 on Care and Protection of living animals undergoing experimental or other scientific procedures; authorization number 17/2010-B, June 30, 2010 and 367/2016-PR]: additionally, an ad hoc Ethical Committee of the University of Turin approved this study. All efforts were made to minimize the number of animals used and their suffering. They were identified by PCR according to Jackson Laboratory's genotyping protocol.

Genotyping mice

DNA from mouse tail was extracted as previously described (Sirabella et al., 2018). On the extracted DNA, we performed PCR in order to evaluate the presence of the human

transgene superoxide dismutase-1 (hSOD1) gene, and these mice were referred as TG. The primers used were: hSOD1 fwd 5'-CATCAGCCCTAATCCATCTGA-3' and hSOD1 rev 5'-CGCGACTAACAATCAAAGTGA-3'.

Behavioral tests

In order to identify the symptom onset and to follow the disease progression, TG mice underwent specific behavioral tests: rotarod and paw grip endurance (PaGE) tests were performed by a trained blind observer, as previously reported (Valsecchi et al., 2013; Boido et al., 2014), starting from the postnatal day 60 (P60), a fully asymptomatic phase of the disease. The first two weeks of tests were considered as training for the animals. The tests were performed twice a week. The body weight was also monitored during the whole period of observation. Briefly, for the Rotarod test we measured the time animals could remain on the rotating cylinder in a 7650 accelerating model of a rotarod apparatus (Ugo Basile, Italy). Each animal was given three trials. The arbitrary cut-off time was 300 sec, and the accelerated speed went from 4 to 32 rpm. For PaGE test the animal was placed on the wire-lid of conventional housing cage: the lid was gently shaken to prompt the mouse to hold onto the grid before it was swiftly turned upside down. Grip score was measured as the length of time that the mouse was able to hang on to the grid. The arbitrary cut-off time was 90 sec. This G93A stock of mice has a high transgene number, and shows the first symptoms of disease approximately at 3 months of age, with a rapid progression of the disease in 1 month. We considered three groups of animals: a) asymptomatic, mice between 2 and 3 months of age, that do not display any motor performance deficit; b) early symptomatic, animals that displayed decreased motor behavioral performance in two consecutive testing sessions, approximately at 3.5 months of age; c) late symptomatic, mice of 4 and 4.5 months of age whose motor conditions are seriously compromised as previously reported.

RT-PCR analysis for:

ALS patients

Peripheral whole blood samples from ALS patients and HC were collected into a Tempus Blood RNA Tubes (Thermos Fisher) and stored at -80°C until use. Total RNA from was automatically extracted using the Maxwell RSC Station and products (Promega), following the manufacturer's instructions and was reverse-transcribed at final concentration of 20 ng/µL using the RT High Capacity Transcription Kit following the manufacturer's instructions (Life Technologies).

Mice

Mice were deeply anaesthetized with 3% isoflurane vaporized in O_2/N_2O 50:50 and sacrificed. The blood was rapidly collected in Tempus Blood RNA Tubes (Thermos Fisher) and stored at -80°C until use. Total RNA from was automatically extracted using the Maxwell RSC Station and products (Promega), following the manufacturer's instructions and was reverse-transcribed at final concentration of 20 ng/µL (Thermos Fisher), using the RT High Capacity Transcription Kit following the manufacturer's instructions (Life Technologies). The spinal cord was rapidly removed and immediately frozen on dry ice and stored at -80° C until use. Total RNA was extracted with Trizol, following supplier's instructions (Life Technologies) and cDNA was synthesized using 2 µg of total RNA with the High Capacity Transcription Kit following supplier's instruction (Life Technologies) as previously reported (Sisalli et al., 2014; Formisano et al., 2015).

Gene expression analysis was performed by real-time PCR using Applied Biosystems' TaqMan gene expression products (Life Technology). For HC and ALS patients, primers from Applied Biosystems' TaqMan Assay-on-demand-TM gene expression products were used: glyceraldehyde-3-phosphate dehydrogenase, (GAPDH; Hs99999905_m1) and Nurr1 (Hs00428691_m1) (Life Technologies). For mice Applied Biosystems' TaqMan gene expression assay Nurr1 (TaqMan ID: Mm00443060_m1) and GAPDH (ID: Mm99999915_g1) were used as previously reported (Valsecchi et al., 2015). Expression levels of target genes were calculated by the normalized comparative cycle threshold (Ct) method (2^−ΔΔCt), using GAPDH as reference gene and the Universal Human Reference RNA (Stratagene) as calibrator for human samples. For blood murine samples expression levels of target genes were calculated by the normalized comparative cycle threshold (Ct) method (2^−ΔCt), using GAPDH as reference gene.

Western blot

Nuclear and cytoplasmic extracts were obtained as previously described (Guglielmotto et al., 2014; Piras et al., 2017). Briefly, samples (spinal cord) were first washed with cold phosphate-buffered saline and then homogenated with a 28-gauge needle syringe in ice-cold lysis buffer (10 mM Hepes pH 7.9, 10 mM KCl, 1.5 mM $MgCl_2$, 0.1 mM EGTA, 0.2mM PMSF, 10 mM NaF, 1 mM Na_3VO_4, 0.5 g/ml apronitin, 1 g/ml leupeptin, 1 g/ml pepstatin). Tissues were allowed to swell on ice for 10 min, vortexed and collected by centrifuge. The supernatant was discarded and the pellet dissolved in ice cold buffer (20 mM Hepes pH 7.9, 400 mM NaCl, 1.5 mM $MgCl_2$, 0.1 mM EGTA, 0.2mM PMSF, 10 mM NaF, 1 mM Na_3VO_4, 0.5 g/ml apronitin, 1 g/ml leupeptin, 1 g/ml pepstatin) and incubated on ice for 30' min for

high salt extraction. Cellular debrisis was removed by centrifugation and the supernatant fraction stored at -80°C.

Protein concentration was determined by the Bio-Rad protein assay (Biorad). To detect the proteins of interest, specific antibodies were used: anti-Nurr1 (mouse monoclonal antibody, 1:750; Santa Cruz) and anti-lamin A (rabbit polyclonal, 1:1000; Swant). Immunoreaction was revealed using antimouse and antirabbit immunoglobulin G conjugated to peroxidase 1:2000 (GE Healthcare) by the ECL reagent (GE Healthcare). The optical density of the bands was determined by Chemi Doc Imaging System (Biorad) and normalized to the optical density of lamin A.

Chromatin Immunoprecipitation Assay

The chromatin immunoprecipitation assay and quantitative real-time polymerase chain reaction (qPCR) quantification were performed as previously described (Valsecchi et al., 2013; Guida et al., 2017; 2018, Iannello et al., 2019). In particular, tissues were cross-linked with 1% formaldehyde in PBS for 10 min at 37°C. The reaction was stopped by adding glycine to a final concentration of 125 mM at room temperature (RT). Crosslinked spinal cords were washed three times in cold PBS containing proteinase inhibitors and then collected in 1 ml of cell lysis buffer (5 mM Pipes pH 8, 85 mM KCl and 0.5% NP-40). After 10 min of incubation on ice, nuclei were collected by centrifugation and lysed with 400 µl of nuclei lysis buffer (50 mM Tris-HCl pH 8, 10 mM EDTA and 1% SDS). The lysates were incubated on ice for 10 min and then sonicated 20 times for 20 sec at 30% amplitude with SonoPlus HD2070 sonicator (Bandelin). Small portion of sonicated chromatin (25 µl) was used to verify that the average size of DNA fragments was in the range of 250–500 bp. 1 µg of sheared chromatin for each immunoprecipitation was diluted in IP buffer (16.7 mM Tris-HCl pH 8, 167 mM NaCl, 1.2 mM EDTA, 0.01% SDS, 1.1% Triton X100) and incubated with 0.5 µg of antibodies against Nurr1 and NFkB p65 (cat. numbersc-990 and sc-372, respectively; Santa Cruz Biotechnology), histones H3K4me3 and H3K27me3 (cat.numbers 39915 and 39155, respectively; Active Motif) in a BSA pre-treated 96-well dish at 4°C overnight on an orbital shaker. Samples with IgG antibody (cat. number sc-2027; Santa Cruz Biotechnology) were run in parallel as negative controls. The following day, 30 µl of 50% Protein A Sepharose™ 4 Fast Flow (GE Healthcare) slurry was added and incubated for 2 hrs at 4°C to capture the immune complexes. Proteins and DNA not specifically associated with the beads were removed by sequentially washing with low-salt buffer (0.1% SDS, 1% Triton X-100, 2 mM EDTA, 20 mM Tris-HCl pH 8 and 150 mM NaCl), high-salt buffer (0.1% SDS, 1% Triton X-100, 2 mM EDTA, 20 mM Tris-HCl, pH 8 and 500 mM NaCl), LiCl washing

buffer (0.25 M LiCl; 1% deoxycholate sodium salt, 1 mM EDTA, 10 mM Tris-HCl pH 8 and 1% NP-40) and twice with Tris-EDTA buffer (10 mM TrisHCl pH 8, 1 mM EDTA) at 4°C for 5 min each wash. The immunoprecipitated DNA-protein complexes were purified using 10% Chelex® 100 Resin (BioRad) for 10 min at 95°C. Proteins were digested by incubating each sample with 20 µg of Proteinase K (Thermo Fisher Scientific) for 30 min at 55°C and then 10 min at 95°C to obtain Proteinase K inactivation, thus achieving DNA purification.

Quantification of ChIP enriched DNA was performed by real-time PCR using iTaq Universal SYBR Green Supermix (Bio-Rad). The enrichment of target sequence in the immunoprecipitated samples was normalized on input samples (1% of total chromatin used per IP) and expressed as the ratio between WT and TG binding enrichment on iNOS promoter for each transcriptional factor. Custom ChIP primers were: iNOS promoter forward: 5'-ATGCCATGTGTGAAAATTCC-3' and reverse: 5'-TGGGCTAGCCTGGTCTACAG-3'. Samples were amplified simultaneously in triplicate in one assay run.

Immunofluorescence

Immunostaining procedures on spinal cord sections were performed as previously described (Boido et al., 2014; 2018). Briefly, animals (TG n=3, WT n=3, for every analyzed phase) were deeply anaesthetized by gaseous anesthesia (3% isoflurane vaporized in O_2/N_2O 50:50) to undergo intracardiac perfusion with 4% PAF pH 7.4. The lumbar spinal cords were removed and post-fixed in PFA for 2 hrs at 4°C. Samples were transferred overnight into 30% sucrose in 0.1 M phosphate buffer at 4°C for cryoprotection, embedded in cryostat medium (Killik; Bio-Optica) and cut on the cryostat (Microm HM 550) in serial transverse 14 µm-thick sections, kept in PBS at 4°C or mounted onto gelatin-coated slides, to be processed for immunostaining. After unspecific binding sites were blocked for 30 min at room temperature with 2% Triton X-100 and 10% normal donkey serum (Sigma-Aldrich) in PBS, pH 7.4, the sections were incubated in the same solution with the following primary antibodies at 4°C overnight: 1:100 polyclonal rabbit anti-Nurr1 (cat. number sc991; Santa Cruz); 1:1000 monoclonal mouse anti-Neurofilament H Non-Phosphorylated (SMI 32R; cat. number 14974402; Covance); 1:1000 monoclonal mouse anti-glial fibrillary acidic protein (GFAP; cat. number ab190288; Abcam); 1:1000 polyclonal rabbit anti-IBA1 (cat number 019-19741; Wako Chemicals); 1:1000 monoclonal rat anti mouse CD68 (cat. number MCA1957; Bio-Rad Laboratories S.r.l). The next day sections were washed in PBS and incubated in 1:200 cyanine 3-conjugated anti-rabbit, Alexa Fluor® 488anti-mouse (1:200; respectively cat. number 711-165-152 and 715-546-150; Jackson, West Grove, PA, USA) or anti-rat (1:200; cat. number ab150153; Abcam) secondary antibodies, according to the

primary antibodies. Sections were then examined with a Leica TCS SP5 confocal laser scanning microscope light. Photomicrographs were eventually manipulated with autocontrast enhancement, by Photoshop CS2 software.

Statistical analysis

Regarding ALS patients, continuous data are presented as medians and ranges and discrete data are given as counts and percentages. Chi square tests were performed to compare groups of categorical data. Student's t-test or Mann–Whitney U test were used to compare continuous data as appropriate. The correlation between NURR1 gene expression levels and clinical and demographical variables was assessed by Pearson correlations and fitting linear models. In particular, we considered (Table 1): I) sex and age at sampling for all the groups; II) the age at the disease onset. Data obtained from mice were expressed as mean ± standard error (SEM). Statistically significant differences among means and/or ratios were determined by two-way ANOVA test followed by Bonferroni test. Statistical significance was considered at $p\text{-value}<0.05$. All analyses were carried out using R version 3.02and GraphPad Prism 5 software (GraphPad Software, San Diego, CA).

Authors contribution

V.V. and M.B. conceived and designed the study; V.V. performed RT-PCR experiments on mice sample; M.B., N.G. and E.S, performed the immunostaining experiments; F.M., S.P. and S.M. performed RT-PCR on human and murine blood samples; S.C. and A.I. performed ChIP-qPCR experiments; M.G. performed WB assay; V.V., M.B., F.M. and A.V. wrote the manuscript. All authors revised and approved the manuscript prior to submission.

Declaration of Competing Interest

The authors have declared that no conflict of interest exists.

ACKNOWLEDGMENT

This work was supported by University of Turin ("Ricerca Locale 2014, 2015, 2016-2017") grant to MB, and by Ministero dell'Istruzione, dell'Università e della Ricerca-MIUR project "Dipartimenti di eccellenza 2018-2022" to Dept. of Neuroscience "Rita Levi Montalcini", University of Turin.

REFERENCES

Aarnisalo, P., et al., 2002. Defining requirements for heterodimerization between the retinoid X receptor and the orphan nuclear receptor Nurr1. J Biol Chem. 277, 35118-23.

Alvarez-Castelao, B., et al., 2013b. The N-terminal region of Nurr1 (a.a 1-31) is essential for its efficient degradation by the ubiquitin proteasome pathway. PLoS One. 8, e55999.

Anzilotti, S., et al., 2018. Preconditioning, induced by sub-toxic dose of the neurotoxin L-BMAA, delays ALS progression in mice and prevents Na. Cell Death Dis. 9, 206.

Barneda-Zahonero, B., et al., 2012. Nurr1 protein is required for N-methyl-D-aspartic acid (NMDA) receptor-mediated neuronal survival. J Biol Chem. 287, 11351-62.

Baron, O., et al., 2012. Cooperation of nuclear fibroblast growth factor receptor 1 and Nurr1 offers new interactive mechanism in postmitotic development of mesencephalic dopaminergic neurons. J Biol Chem. 287, 19827-40.

Boido, M., et al., 2018. Increasing Agrin Function Antagonizes Muscle Atrophy and Motor Impairment in Spinal Muscular Atrophy. Front Cell Neurosci. 12, 17.

Boido, M., et al., 2014. Human mesenchymal stromal cell transplantation modulates neuroinflammatory milieu in a mouse model of amyotrophic lateral sclerosis. Cytotherapy. 16, 1059-72.

Bonta, P. I., et al., 2006. Nuclear receptors Nur77, Nurr1, and NOR-1 expressed in atherosclerotic lesion macrophages reduce lipid loading and inflammatory responses. Arterioscler Thromb Vasc Biol. 26, 2288-94.

Chia, R., et al., 2018. Novel genes associated with amyotrophic lateral sclerosis: diagnostic and clinical implications. Lancet Neurol. 17, 94-102.

Chiu, I. M., et al., 2008. T lymphocytes potentiate endogenous neuroprotective inflammation in a mouse model of ALS. Proc Natl Acad Sci U S A. 105, 17913-8.

Cozzolino, M., et al., 2012. Amyotrophic lateral sclerosis: new insights into underlying molecular mechanisms and opportunities for therapeutic intervention. Antioxid Redox Signal. 17, 1277-330.

De Miranda, B. R., et al., 2015. The Nurr1 Activator 1,1-Bis(3'-Indolyl)-1-(p-Chlorophenyl)Methane Blocks Inflammatory Gene Expression in BV-2 Microglial Cells by Inhibiting Nuclear Factor κB. Mol Pharmacol. 87, 1021-34.

Ferraiuolo, L., et al., 2011. Molecular pathways of motor neuron injury in amyotrophic lateral sclerosis. Nat Rev Neurol. 7, 616-30.

Formisano, L., et al., 2015. Sp3/REST/HDAC1/HDAC2 Complex Represses and Sp1/HIF-1/p300 Complex Activates ncx1 Gene Transcription, in Brain Ischemia and in Ischemic Brain Preconditioning, by Epigenetic Mechanism. J Neurosci. 35, 7332-48.

Guglielmotto, M., et al., 2014. Aβ1-42 monomers or oligomers have different effects on autophagy and apoptosis. Autophagy. 10, 1827-43.

Guida, N., et al., 2017. p38/Sp1/Sp4/HDAC4/BDNF Axis Is a Novel Molecular Pathway of the Neurotoxic Effect of the Methylmercury. Front Neurosci. 11, 8.

Guida, N., et al., 2018. The miR206-JunD Circuit Mediates the Neurotoxic Effect of Methylmercury in Cortical Neurons. Toxicol Sci. 163, 569-578.

Gurney, M. E., et al., 1994. Motor neuron degeneration in mice that express a human Cu,Zn superoxide dismutase mutation. Science. 264, 1772-5.

Haidet-Phillips, A. M., et al., 2011. Astrocytes from familial and sporadic ALS patients are toxic to motor neurons. Nat Biotechnol. 29, 824-8.

Henkel, J. S., et al., 2009. Microglia in ALS: the good, the bad, and the resting. J Neuroimmune Pharmacol. 4, 389-98.

Hering, R., et al., 2004. Extended mutation analysis and association studies of Nurr1 (NR4A2) in Parkinson disease. Neurology. 62, 1231-2.

Hooten, K. G., et al., 2015. Protective and Toxic Neuroinflammation in Amyotrophic Lateral Sclerosis. Neurotherapeutics. 12, 364-75.

Iannello, A., et al., 2019. Pregnancy Epigenetic Signature in T Helper 17 and T Regulatory Cells in Multiple Sclerosis. Front Immunol. 9, 3075.

Ilieva, H., et al., 2009. Non-cell autonomous toxicity in neurodegenerative disorders: ALS and beyond. J Cell Biol. 187, 761-72.

Kadkhodaei, B., et al., 2013. Transcription factor Nurr1 maintains fiber integrity and nuclear-encoded mitochondrial gene expression in dopamine neurons. Proc Natl Acad Sci U S A. 110, 2360-5.

Kadkhodaei, B., et al., 2009. Nurr1 is required for maintenance of maturing and adult midbrain dopamine neurons. J Neurosci. 29, 15923-32.

Kim, D. H., et al., 2013. Histone H3K27 trimethylation inhibits H3 binding and function of SET1-like H3K4 methyltransferase complexes. Mol Cell Biol. 33, 4936-46.

Le, W., et al., 2008. Decreased NURR1 gene expression in patients with Parkinson's disease. J Neurol Sci. 273, 29-33.

Le, W. D., et al., 2003. Mutations in NR4A2 associated with familial Parkinson disease. Nat Genet. 33, 85-9.

Lee, Y. W., et al., 2012. A novel nuclear FGF Receptor-1 partnership with retinoid and Nur receptors during developmental gene programming of embryonic stem cells. J Cell Biochem. 113, 2920-36.

Liu, H., et al., 2017. NR4A2 genetic variation and Parkinson's disease: Evidence from a systematic review and meta-analysis. Neurosci Lett. 650, 25-32.

Liu, H., et al., 2012. Decreased NURR1 and PITX3 gene expression in Chinese patients with Parkinson's disease. Eur J Neurol. 19, 870-5.

Maira, M., et al., 1999. Heterodimerization between members of the Nur subfamily of orphan nuclear receptors as a novel mechanism for gene activation. Mol Cell Biol. 19, 7549-57.

McCauley, M. E., Baloh, R. H., 2019. Inflammation in ALS/FTD pathogenesis. Acta Neuropathol. 137, 715-730.

McCombe, P. A., Henderson, R. D., 2011. The Role of immune and inflammatory mechanisms in ALS. Curr Mol Med. 11, 246-54.

McMorrow, J. P., Murphy, E. P., 2011. Inflammation: a role for NR4A orphan nuclear receptors? Biochem Soc Trans. 39, 688-93.

Montarolo, F., et al., 2015. Nurr1 reduction influences the onset of chronic EAE in mice. Inflamm Res. 64, 841-4.

Montarolo, F., et al., 2016. Altered NR4A Subfamily Gene Expression Level in Peripheral Blood of Parkinson's and Alzheimer's Disease Patients. Neurotox Res. 30, 338-44.

Montarolo, F., et al., 2014. Effects of isoxazolo-pyridinone 7e, a potent activator of the Nurr1 signaling pathway, on experimental autoimmune encephalomyelitis in mice. PLoS One. 9, e108791.

Murdock, B. J., et al., 2015. The dual roles of immunity in ALS: injury overrides protection. Neurobiol Dis. 77, 1-12.

Murdock, B. J., et al., 2017. Correlation of Peripheral Immunity With Rapid Amyotrophic Lateral Sclerosis Progression. JAMA Neurol. 74, 1446-1454.

Pasinelli, P., Brown, R. H., 2006. Molecular biology of amyotrophic lateral sclerosis: insights from genetics. Nat Rev Neurosci. 7, 710-23.

Piras, A., et al., 2017. Inhibition of autophagy delays motoneuron degeneration and extends lifespan in a mouse model of spinal muscular atrophy. Cell Death Dis. 8, 3223.

Renton, A. E., et al., 2014. State of play in amyotrophic lateral sclerosis genetics. Nat Neurosci. 17, 17-23.

Robberecht, W., Philips, T., 2013. The changing scene of amyotrophic lateral sclerosis. Nat Rev Neurosci. 14, 248-64.

Rodríguez-Calvo, R., et al., 2017. The NR4A subfamily of nuclear receptors: potential new therapeutic targets for the treatment of inflammatory diseases. Expert Opin Ther Targets. 21, 291-304.

Ruiz-Sánchez, E., et al., 2017. Association of polymorphisms and reduced expression levels of the NR4A2 gene with Parkinson's disease in a Mexican population. J Neurol Sci. 379, 58-63.

Safe, S., et al., 2016. Nuclear receptor 4A (NR4A) family - orphans no more. J Steroid Biochem Mol Biol. 157, 48-60.

Saijo, K., et al., 2009. A Nurr1/CoREST pathway in microglia and astrocytes protects dopaminergic neurons from inflammation-induced death. Cell. 137, 47-59.

Saini, A., et al., 2016. Nuclear receptor expression atlas in BMDCs: Nr4a2 restricts immunogenicity of BMDCs and impedes EAE. Eur J Immunol. 46, 1842-53.

Saucedo-Cardenas, O., et al., 1998. Nurr1 is essential for the induction of the dopaminergic phenotype and the survival of ventral mesencephalic late dopaminergic precursor neurons. Proc Natl Acad Sci U S A. 95, 4013-8.

Sekiya, T., et al., 2011. The nuclear orphan receptor Nr4a2 induces Foxp3 and regulates differentiation of CD4+ T cells. Nat Commun. 2, 269.

Sekiya, T., et al., 2013. Nr4a receptors are essential for thymic regulatory T cell development and immune homeostasis. Nat Immunol. 14, 230-7.

Sirabella, R., et al., 2018. Ionic Homeostasis Maintenance in ALS: Focus on New Therapeutic Targets. Front Neurosci. 12, 510.

Sisalli, M. J., et al., 2014. Endoplasmic reticulum refilling and mitochondrial calcium extrusion promoted in neurons by NCX1 and NCX3 in ischemic preconditioning are determinant for neuroprotection. Cell Death Differ. 21, 1142-9.

Thonhoff, J. R., 2018. Neuroinflammatory mechanisms in amyotrophic lateral sclerosis pathogenesis. Curr Opin Neurol. 31, 635-639.

Troost, D., et al., 1990. Immunohistochemical characterization of the inflammatory infiltrate in amyotrophic lateral sclerosis. Neuropathol Appl Neurobiol. 16, 401-10.

Valsecchi, V., et al., 2015. Expression of Muscle-Specific MiRNA 206 in the Progression of Disease in a Murine SMA Model. PLoS One. 10, e0128560.

Valsecchi, V., et al., 2013. Transcriptional regulation of ncx1 gene in the brain. Adv Exp Med Biol. 961, 137-45.

Vercelli, A. et al., 2008. Human mesenchymal stem cell transplantation extends survival, improves motor performance and decreases neuroinflammation in mouse model of amyotrophic lateral sclerosis. Neurobiol Dis. 31, 395-405.

Volakakis, N., et al., 2010. NR4A orphan nuclear receptors as mediators of CREB-dependent neuroprotection. Proc Natl Acad Sci U S A. 107, 12317-22.

Wang, Z., et al., 2003. Structure and function of Nurr1 identifies a class of ligand-independent nuclear receptors. Nature. 423, 555-60.

Won, H. Y., Hwang, E. S., 2016. Transcriptional modulation of regulatory T cell development by novel regulators NR4As. Arch Pharm Res 39, 1530-1536.

Worms, P. M., 2001. The epidemiology of motor neuron diseases: a review of recent studies. J Neurol Sci. 191, 3-9.

Zhang, R., et al., 2005. Evidence for systemic immune system alterations in sporadic amyotrophic lateral sclerosis (sALS). J Neuroimmunol 159, 215–224.

Zetterström, R. H., et al., 1997. Dopamine neuron agenesis in Nurr1-deficient mice. Science. 276, 248-50.

Zhao, W., et al., 2013. Immune-mediated mechanisms in the pathoprogression of amyotrophic lateral sclerosis. J Neuroimmune Pharmacol. 8, 888-99.

Zhou, J., et al., 2010. High-efficiency induction of neural conversion in human ESCs and human induced pluripotent stem cells with a single chemical inhibitor of transforming growth factor beta superfamily receptors. Stem Cells. 28, 1741-50.

Figures

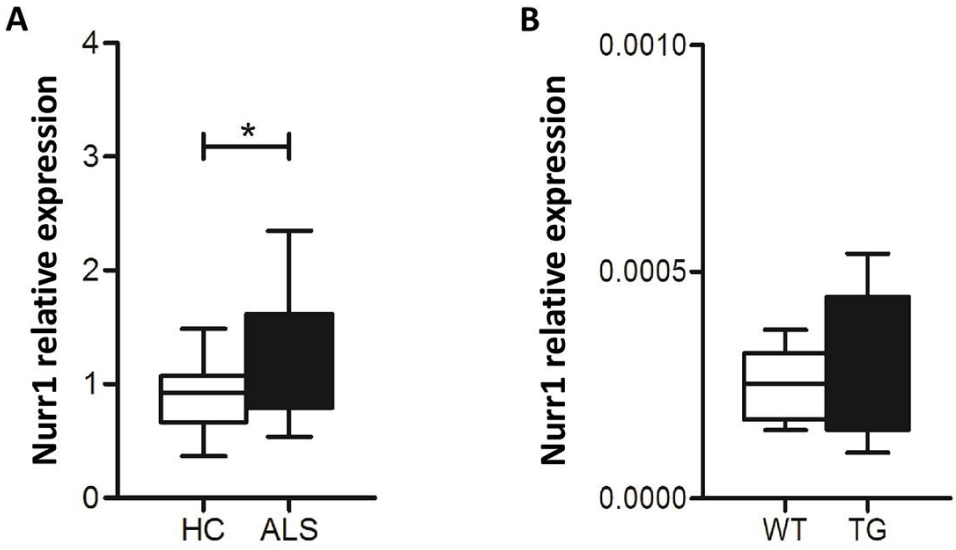

Figure 1. Whole peripheral blood gene expression levels of Nurr1 in ALS patients and in SOD1-G93A mice.

A, Comparison of gene expression levels of Nurr1 among 43 ALS and 41 HC. Nurr1 is up-regulated in ALS patients compared to HC (t-test, p=0.01). Relative expression was calculated using the normalized comparative cycle threshold (Ct) method (2^-ΔCt). **B,** Comparison of gene expression levels of Nurr1 among 7 WT and 8 TG mice. No differences were detected for Nurr1 in TG mice compared to HC (t-test, p=0.69). Relative expression was calculated using the normalized comparative cycle threshold (Ct) method (2^-ΔCt).

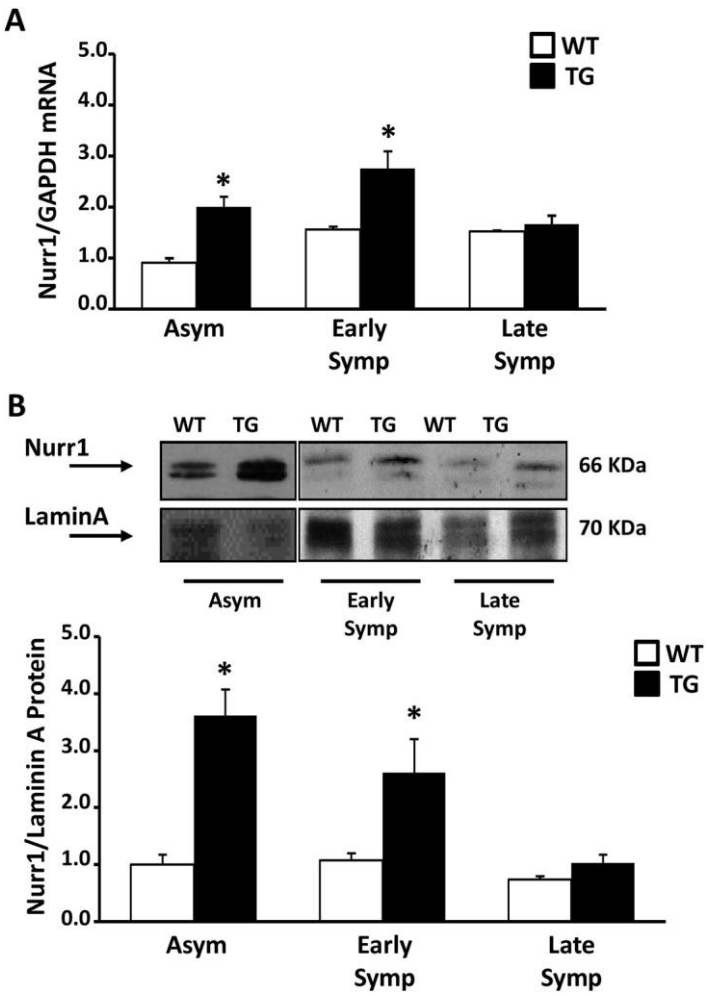

Figure 2. Nurr1 mRNA and protein was up-regulated in the spinal cord of asymptomatic and early symptomatic SOD1-G93A mice.

A, mRNA expression levels of Nurr1 in the spinal cord of asymptomatic (Asym, n=11), early symptomatic (Early Symp, n=5) and late symptomatic (Late Symp, n=4) SOD1-G93A (TG, black columns) animals, compared to age matched WT (white columns) mice. GAPDH gene was used as endogenous control. **B,** Representative Western blot displaying the expression levels of Nurr1 protein in nuclear extracts from spinal cord of Asym (n=8), Early (n=5) and Late Symp (n=3) TG and WT animals. The graph below the image reports the quantification of Nurr1, expressed as ratio with the endogenous control laminA.

Each column represents the mean ± SEM. Statistically significant differences among means were determined by two-way ANOVA followed by Bonferroni test. *p<0.05 TG vs respective WT.

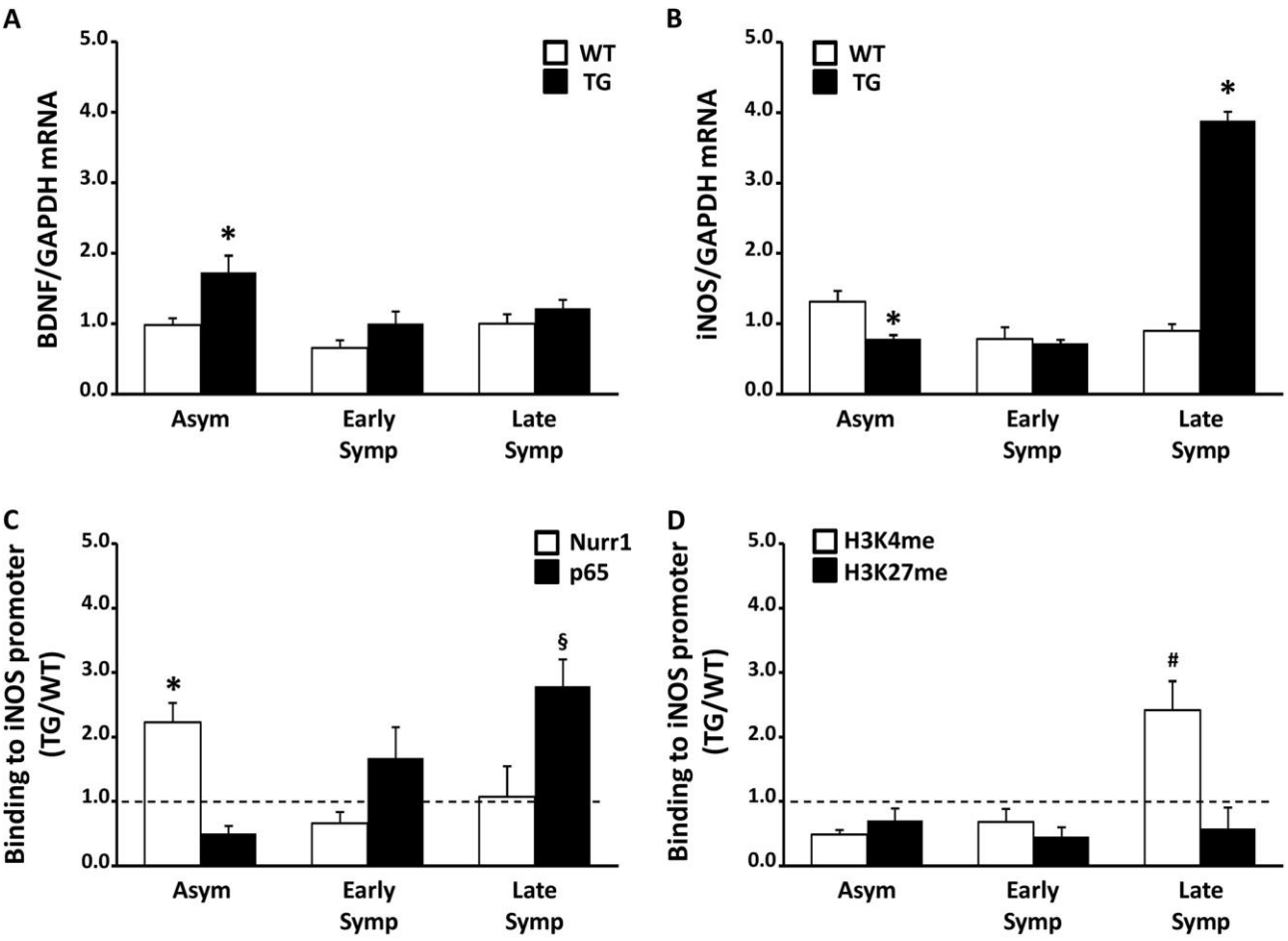

Figure 3. Nurr1 activated BDNF expression and repressed iNOS transcriptional activation by docking NF-kB on iNOS promoter. A-B, mRNA expression levels of BDNF (panel A) and iNOS (panel B) in the spinal cord of asymptomatic (Asym, n=10), early symptomatic (Early Symp, n=5) and late symptomatic (Late Symp, n=3 for panel A and n=4 for panel B) SOD1-G93A (TG, black columns) animals, compared to age matched WT (white columns) mice. GAPDH gene was used as endogenous control. Each column represents the mean ± SEM. Statistically significant differences among means were determined by two-way ANOVA followed by Bonferroni test. *p<0.05 TG vs respective WT. **C-D,** ChIP analysis of Nurr1 and p65 (panel C), and H3K4me and H3K27me (panel D) on iNOS promoter in the spinal cord of Asym, Early Symp and Late Symp TG and WT animals. The binding activity of each transcriptional factor was calculated as the percentage of total input of chromatin DNA and represented as the ratio between TG and age matched WT animals. Each column represents the mean ± SEM (n=3). Statistically significant differences among means were determined by two-way ANOVA followed by Bonferroni test *p<0.05 Nurr1 vs p65; §p<0.05 p65 vs Nurr1; #p<0.005 H3K4me vs H3K27me.

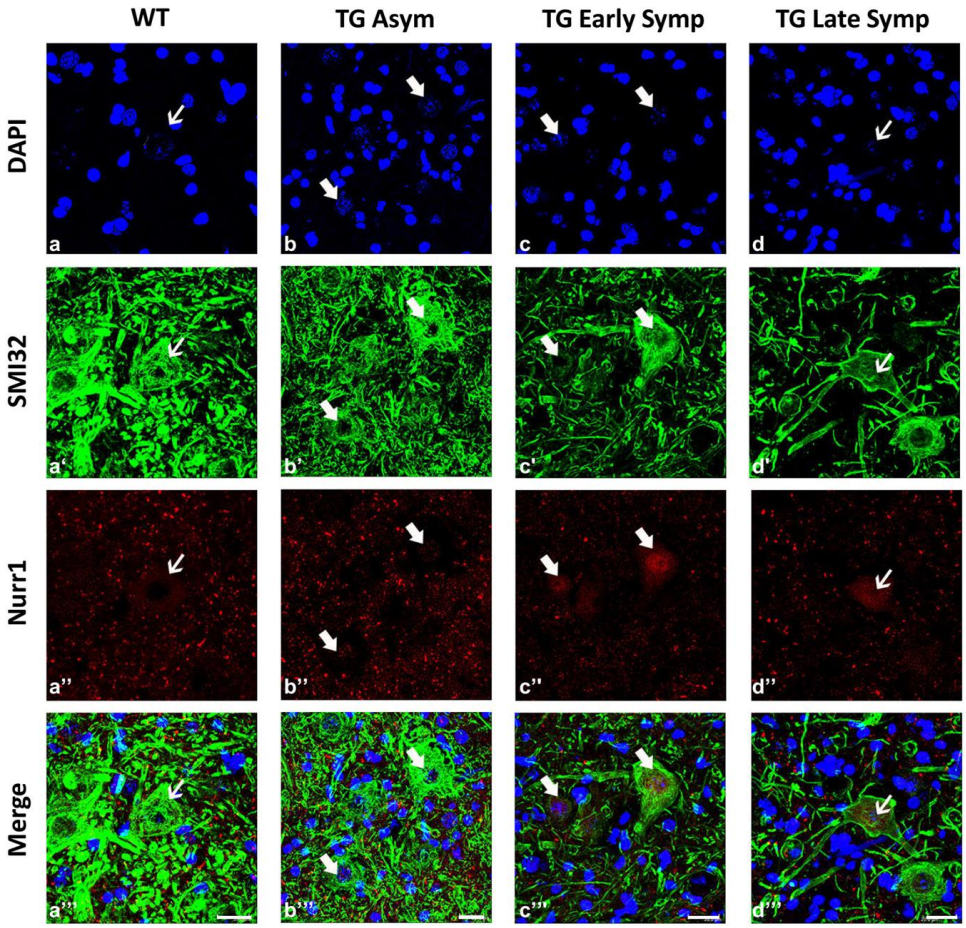

Figure 4. Nurr1 protein is expressed in MNs of TG animals.

A, representative confocal images showing the double labelling of Nurr1 (red) and SMI32 (green) in lumbar spinal cord of WT animals (a-a'''), and Asym (b-b'''), Early Symp (c-c'''; e-e''') and Late Symp (d-d''') TG mice. Nuclei are labelled with DAPI (blue). Thin arrows show mainly cytoplasmic localization of Nurr1, while thick arrows indicate nuclear localization of Nurr1 in MNs. Scale bar=20 μm.

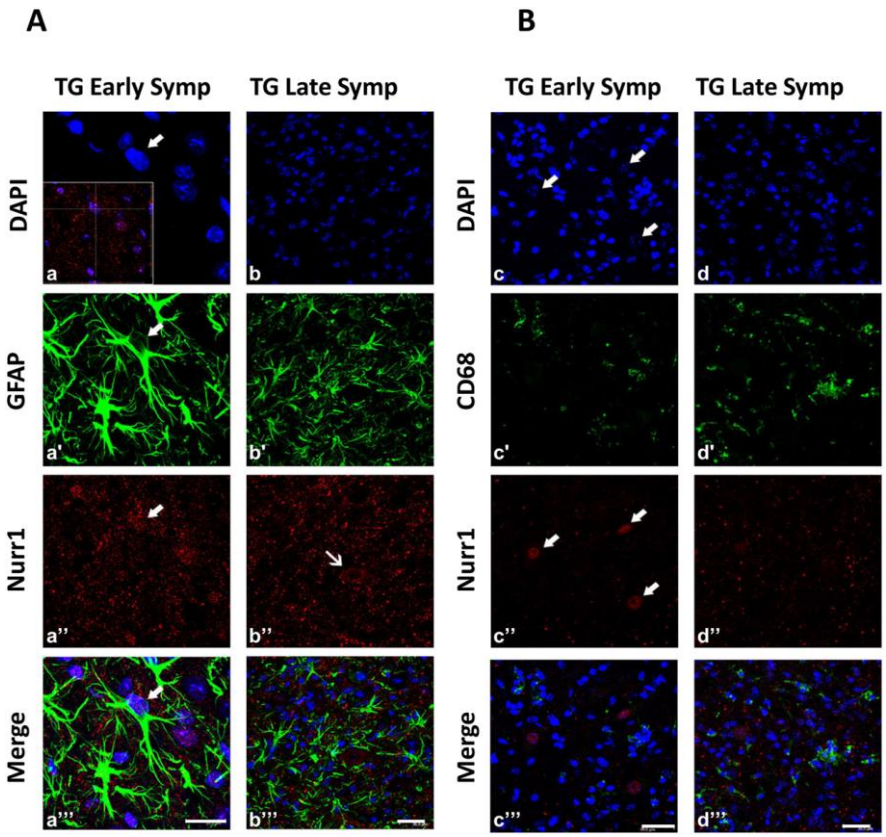

Figure 5. Nurr1 protein is expressed in astrocytes of TG animals.

A-B, representative confocal images showing the double labelling of Nurr1 (red) and GFAP (green, panel A) or CD68 (green, panel B) in lumbar spinal cord of Early Symp (a-a'''; c-c'''), and Late Symp (b-b'''; d-d''') TG mice. Nuclei are labelled with DAPI (blue). Thin arrows show mainly cytoplasmic localization of Nurr1, while thick arrows indicate nuclear localization of Nurr1 in astrocytes: in a inset, rotations along the x- and y-axes show the superposition of the two colors on the z-axis. In b'' (TG, Late Symp), it is evident that the astrocytes are not labeled, but they surround a presumable Nurr1-positive MN (Nurr1 expression at the cytoplasmic level, thin arrow). Panel B demonstrates the absence of Nurr1-positive microglial cells, instead further confirming its expression in plausible MNs (thick arrows). Scale bar=20 μm in a-a''', and 30 μm in b-b''', c-c''', d-d'''.

Table 1. Demographic and clinical characteristics of the enrolled populations.

	HC (n=41)	ALS (n=43)	*Pvalue*
Age at time of sampling (y), mean (SD)	56.7 (10.97)	64.6 (12.03)	0.002[a]
Sex, F (%)	23 (56.1)	19 (44.2)	0.38[b]
Age at disease onset (y), mean (SD)	-	61.98 (11.98)	-
Patients treated with specific therapies, n (%)	-	3 (7.1) None 14 (33.3) Riluzole 22 (52.4) Riluzole + other drugs[c] 3 (7.1) Other drugs[c]	-
fALS patients with known mutations, n (%)		7 (16,3): 4 C9Orf72, 2 SOD1, 1 TARDP43	
sALS patients with known mutations, n (%)		36 (83,7): 1 C9Orf72, 1 SOD1, 1 OPTN	

HC, healthy controls; ALS, amyotrophic lateral sclerosis; y, years; F, female.

[a] t-test

[b] Fisher exact test

[c] Other drugs (L-acetilcarnitine, tocopherol, chininum sulphuricum, baclofene, gabapentin, pregabalin, pyridostigmine bromide, escitalopram, citalopram, palmitoylethanolamide)

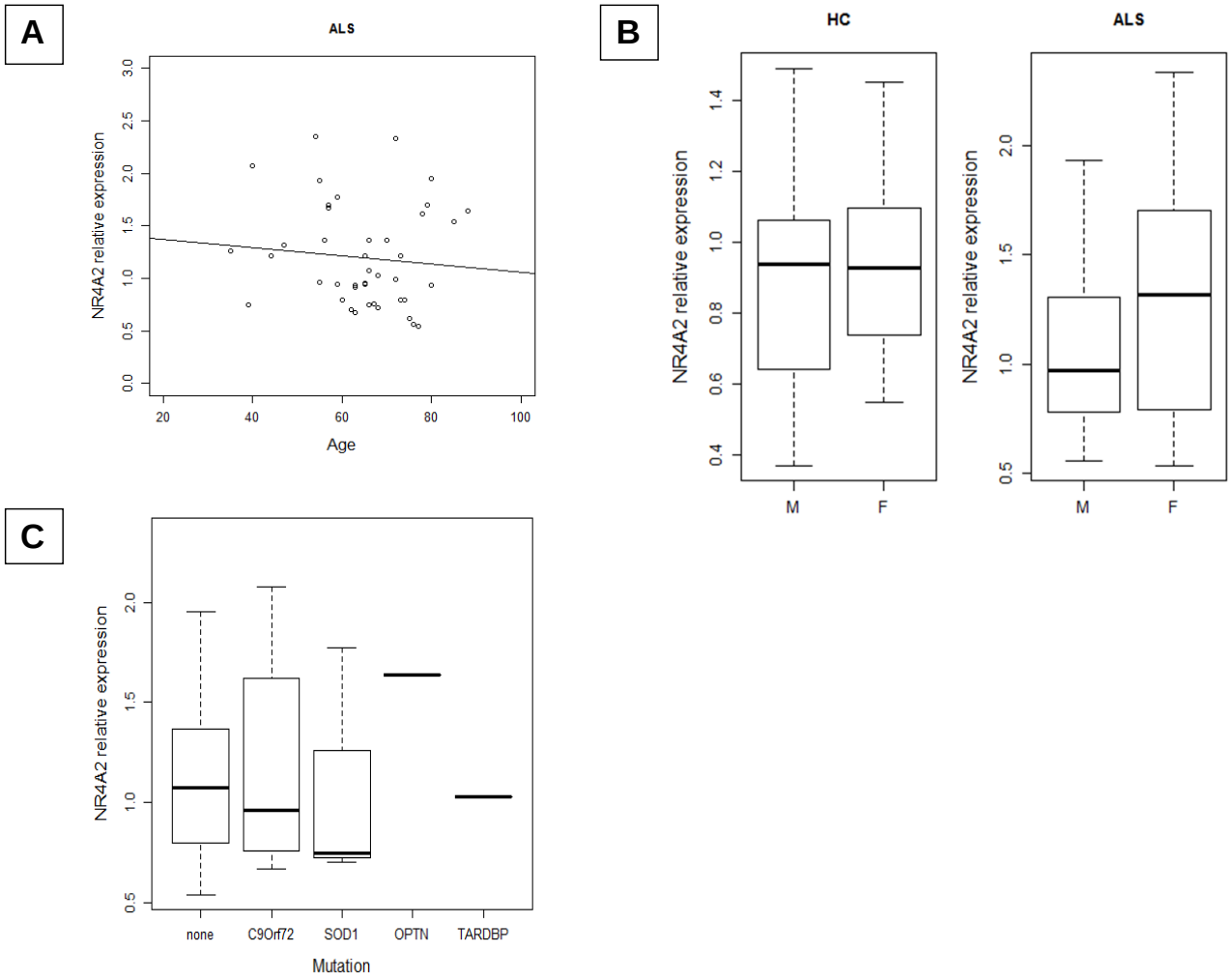

Figure S1. Correlation between Nurr1 expression levels and age, gender and mutations in ALS patients.

A, there is no correlation between Nurr1 expression levels and age of ALS patients (Pearson correlation coefficient r=-0.09, p=0.55). **B**, there are no significant differences in Nurr1 expression between males (M) and females (F) in both HC (t-test, p=0.53) and ALS patients (Mann-Whitney U test, p=0.32). **C**, Nurr1 expression levels for the different mutations identified in fALS and sALS patients. No association between Nurr1 level and the mutations identified was investigated due to the small sample size of each group.

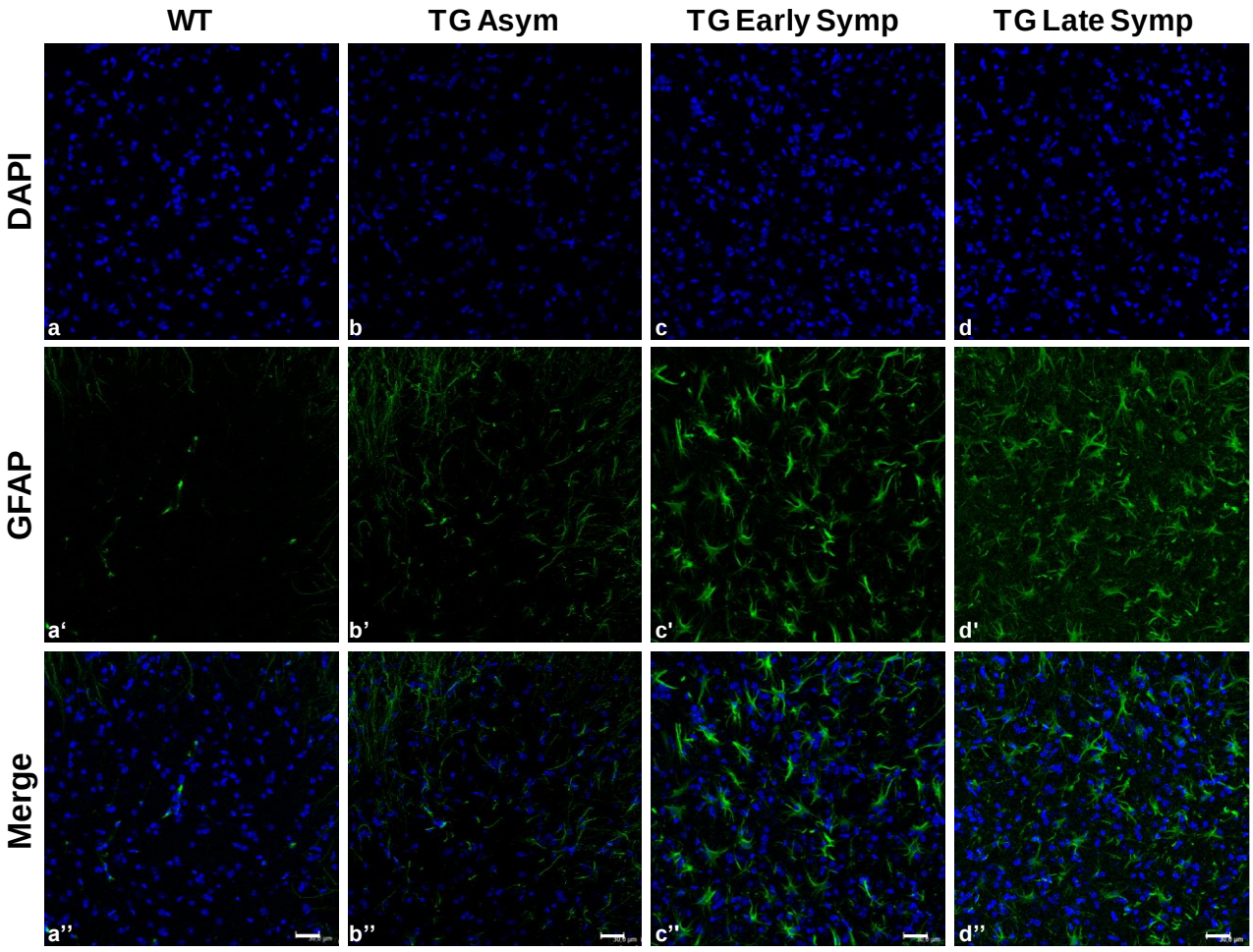

Figure S2. Astrogliosis activation analysis.

Representative confocal images showing reactive astrogliosis in terms of GFAP-labeling (green) in the lumbar spinal cord of WT animals (a-a’’’), and Asym (b-b’’’), Early Symp (c-c’’’) and Late Symp (d-d’’’) TG mice. Nuclei are labelled with DAPI (blue). Scale bar=30 μm.

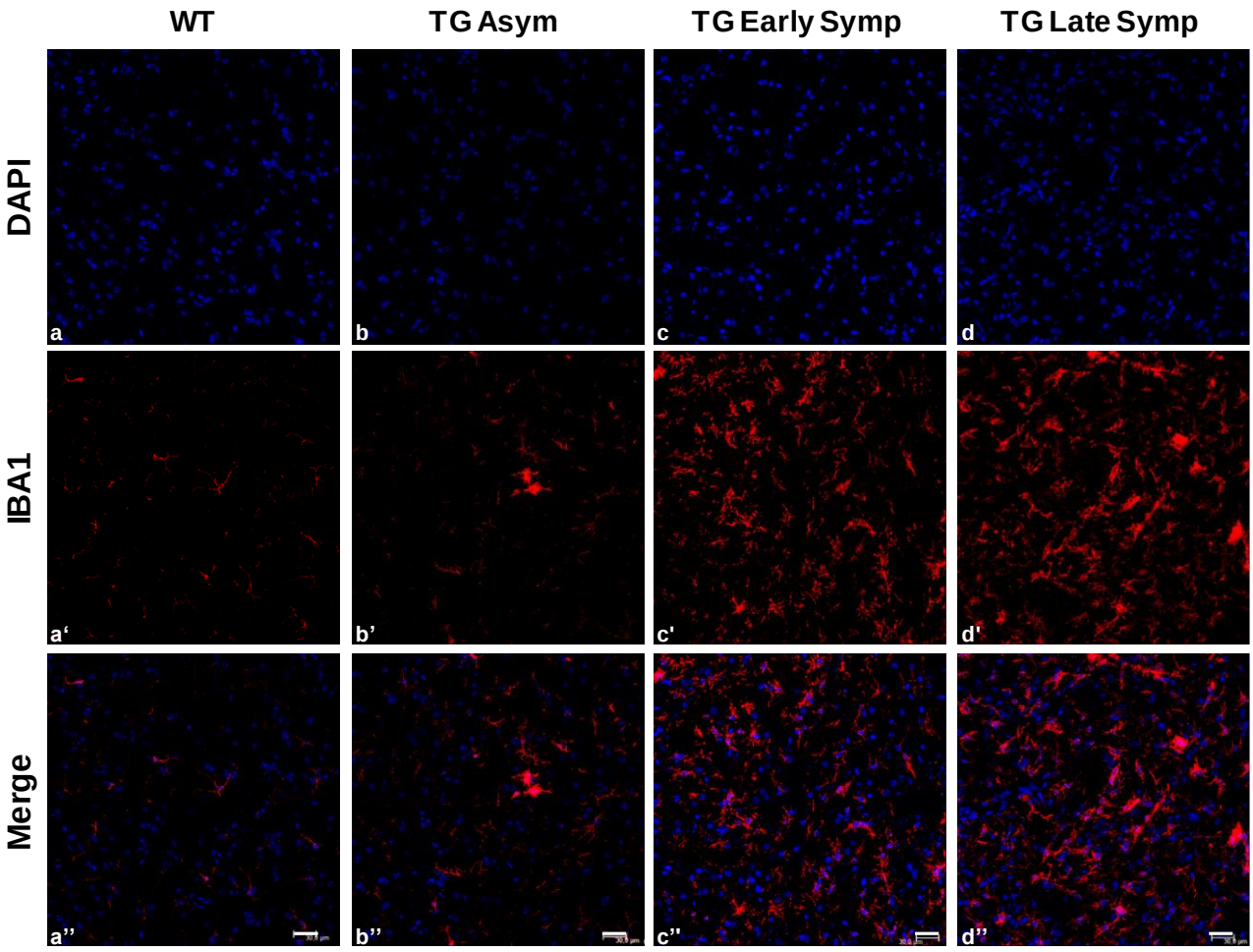

Figure S3. Microglial activation analysis.

Representative confocal images showing microglia activation in terms of IBA1-labeling (red) in the lumbar spinal cord of WT animals (a-a'''), and Asym (b-b'''), Early Symp (c-c''') and Late Symp (d-d''') TG mice. Nuclei are labelled with DAPI (blue). Scale bar= 30μm.